ISSN 0001-4370, Oceanology, 2010, Vol. 50, No. 5, pp. 675–687. © Pleiades Publishing, Inc., 2010.
Original Russian Text © V.I. Burenkov, Yu.A. Goldin, V.A. Artem'ev, S.V. Sheberstov, 2010, published in Okeanologiya, 2010, Vol. 50, No. 5, pp. 716–729.

MARINE PHYSICS

Optical Characteristics of the Kara Sea Derived from Shipborne and Satellite Data

V. I. Burenkov, Yu. A. Goldin, V. A. Artem'ev, and S. V. Sheberstov

Shirshov Institute of Oceanology, Russian Academy of Sciences, Moscow, Russia

E-mail: bur-07@yandex.ru, goldyuri@yandex.ru

Received September 3, 2008; in final form, May 5, 2009

Abstract—Results of optical studies of the Kara Sea waters are considered. The data of ship borne measurements are compared with satellite observations. The maximum values of the beam attenuation coefficient, the chlorophyll, and the yellow substance fluorescence were observed in the Ob gulf and in the coastal waters west of the Yamal Peninsula. The minimum values were observed in the central and western parts of the Kara Sea. Frontal zones with sharp changes of the parameters involved were observed. The distribution of the seawater's optical characteristics was closely related to the hydrological structure of the Kara Sea's waters. The data of the shipborne measurements were consistent with the satellite observations.

DOI: 10.1134/S000143701005005X

1. INTRODUCTION

The comprehensive research of the optical properties of the waters of the Arctic seas of Russia commenced rather recently. In 1991, the first optical measurements took place in the Laptev Sea and, incidentally, in the Kara Sea [3]. The optical properties of the Kara Sea were studied as part of the 49th cruise of the R/V *Dmitriy Mendeleev* in 1993 [4]. The results of the investigation of the light attenuation coefficients of the Kara Sea waters were reported in [11] too. In 1998, the 13th and 14th cruises of the R/V *Akademik Sergey Vavilov* involved optical measurements in the eastern (Pechora Sea) and central regions of the Barents Sea [2]. The collected evidence resulted in basic knowledge of the distribution of the optical properties of the Arctic seas. Among others, the river run-off effect on the spatial structure of the optical fields was studied.

The present paper considers results of the optical measurements as part of the 54th cruise of the R/V *Akademik Mstislav Keldysh* in October of 2007. In contrast to the earlier research, the satellite data from the ocean color scanners (MODIS-Aqua and SeaWiFS) substantially supplemented the shipborne observations, thanks to which we obtained the general pattern of the distribution of the bio-optical features of the Kara Sea and were able to perform targeted shipborne measurements in view of the satellite information, which was helpful in the localization of the frontal zones and the like.

2. INSTRUMENTATION

We used the following means to reveal the optical structure of the regions we studied: (1) the vertical profiling of the attenuation coefficient $C(z)$ at the stations of the TsUM compact universal transmissometers [1]; (2) the underway recording of the fluorescence intensity of the dissolved organic matter (DOM) and the chlorophyll *a* (Chl "*a*") with the help of a PLF flow-through laser fluorometer [8]; (3) the estimation of the depth Z_W of a Secchi disk's visibility at the stations under the daylight conditions.

The TsUM transmissometer measured the attenuation coefficient at the wavelength of 530 nm with an accuracy of 0.02 m^{-1}. Its built-in pressure and temperature sensors were accurate to within 1 m of the depth and 0.1°C, respectively. High precision means were used to calibrate the sensors.

The PLF instrument's specifications involve the wavelength of fluorescence excitation of 337.1 nm; the energy and length of the excitation pulse are 50 μJ and 10 ± 2 ns, respectively; the repetition rate of the excitation pulses is 10 Hz; the maximum sensitivity of the intensity channel falls on the wavelength of 480 nm for the DOM fluorescence and on 685 nm for the chlorophyll channel; the Raman band channel's maximum falls on 380 nm; and the discharge rate of the flow-through system is 5.5 l/min.

Observations in the southern Atlantic Ocean [6] demonstrated the efficiency of the PLF measurements in combination with the satellite data.

The optical observations were performed concurrently with the biological and geological measurements with water sampling for the suspended particle determinations to account for the vertical profiles of the attenuation coefficient; indications of the frontal zones from a flow-through fluorometer served for

choosing the sites of the stations. The satellite information served the same purpose too.

3. THE SATELLITE DATA: THE PROCESSING TECHNIQUE, ALGORITHMS, AND RESULTS

The long-term quasi-continuous satellite observations of the ocean's color make it possible to regularly observe the changes in the structure and functioning of the coastal ecosystems; to monitor the quality of the coastal waters; and to explore the river run-off's propagation, the mezoscale eddies, the position and variability of the frontal zones, and other dynamical phenomena.

In the recent decade, a new understanding of the spatial–temporal structure of the bio-optical parameters' distribution in the seas of Russia emerged thanks to systematic observations with the ocean color scanners SeaWiFS and MODIS-Aqua [10,13–15].

A number of such scanners are presently operating. We used the data of the MODIS-Aqua for the analytical treatment of different bio-optical parameters. The basic advantage of this scanner is the fact that its data become available a day after the instant of the measurements (a 14 day delay is typical of the information from the SeaWiFS scanner). This permits the timely processing of the incoming information and transmitting the latter to a research vessel for the correction of its pathway depending on the specific features of the distributions of the bio-optical parameters retrieved from the satellite data.

To calculate the bio-optical parameters, we used the MODIS-Aqua data of level L2 having a spatial resolution of 1.1 × 1.1 km at the nadir viewing. These materials were downloaded from the HACA GSFC (Goddard Space Flight Center) data center and involve such standard products as the estimates of the normalized water-leaving radiance L_{WN}, the aerosol's optical thickness τ_a, the coefficient of the diffuse light attenuation for the wavelength of 490 nm $K_d(490)$, the chlorophyll concentration C_{chl} according to the standard bio-optical algorithm, and the sea surface's temperature (SST). We used an original Windows-based software package of the SIO RAS for the subsequent data processing. The package incorporates new and improved data treatment algorithms that are helpful in the calculation of the L2 products: the chlorophyll concentration C_{chl} based on the regional algorithms, the backscattering coefficient of the suspended particles at the wavelength of 555 nm $b_{bp}(555)$, and the concentration of the suspended matter. The package permitted us to average the L2 data in space and time (i.e., to obtain data of level 3) and to compute the diverse statistics. The computation resulted in the daily values of the L3 level in bins of 4 × 4 km centered at the nodes of a standard grid. The monthly and other mean distributions were found by averaging the daily L3 data over the respective time period.

According to the earlier ground-truthing measurements in the Barents and White Seas, the standard algorithms for the data processing of the MODIS-Aqua and SeaWiFS data yield substantially overestimated chlorophyll concentrations because of errors in the atmospheric correction and the regional specificity of the bio-optical parameters (the light absorption of the DOM is much stronger than that of the phytoplankton pigments). We developed a regional algorithm for the chlorophyll determination in the Kara Sea waters using both shipborne and satellite data. It is based on the correlation between the measured chlorophyll concentration and the ratio of the water leaving radiances $L_{WN}(531)/L_{WN}(551)$. The satellite data for the Kara Sea are difficult to acquire because of the virtually permanent cloudiness, which resulted in relatively sparse concurrent measurements of the radiance and the chlorophyll. Their correlation was relatively poor. Consequently, we consider our chlorophyll determinations in what follows to be preliminary estimates.

In addition to the standard procedures, we used an original algorithm for the backscattering coefficient of the suspended particles [5] developed for cases when the semi-analytical algorithm fails due to an error in the atmospheric correction, which is typical of the Barents and Kara seas. The "simplified" algorithm involves only two spectral channels (510 and 555 nm for the SeaWiFS, and 531nm and 551 nm for the MODIS), where the correction errors are much lower against the channels centered at 412, 443, and 490 nm. We applied this algorithm to the SeaWiFS channels in [5] but conformably modified it for the spectral channels of the MODIS-Aqua.

The frequent occurrence of cloud cover at high latitudes leaves only fragments of the water's surface available for satellite remote sensing. Because of this, it is often necessary to average the data over a certain time period to obtain a general pattern of the distribution of the bio-optical parameters (specifically, in the Kara Sea).

Figures 1 and 2 give the spatial distributions of the backscattering coefficient of the suspended particles b_{bp} computed from the satellite data and the satellite images of the SST distributions (Fig. 1) and chlorophyll concentrations C_{chl} based on the standard MODIS-Aqua and regional algorithms (Fig. 2) with the data being averaged over the period of September 1–26, 2007. Even with such a long averaging period, the remote sensing data are lacking in some areas of the Kara Sea due to the cloud cover for the whole period (the white color in the satellite images corresponds to these conditions).

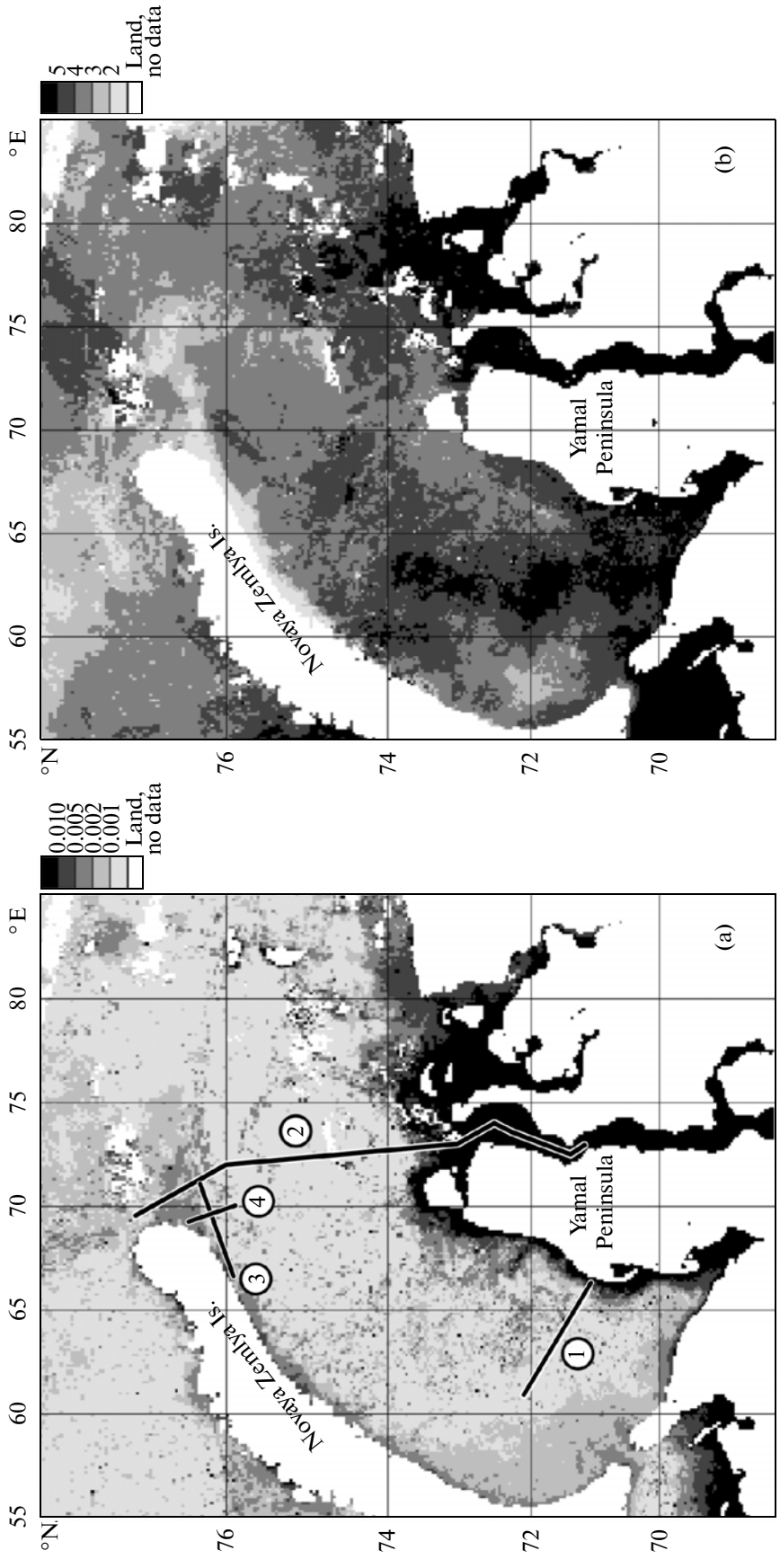

Fig. 1. Spatial distribution of the coefficient of backscattering of light by the suspended matter b_{bp} (a) and SST (b) in the Kara Sea from the data of the MODIS-Aqua ocean color scanner averaged over the period of September 1–26, 2007. The numbered lines designate the sections in which the data presented in the paper were collected.

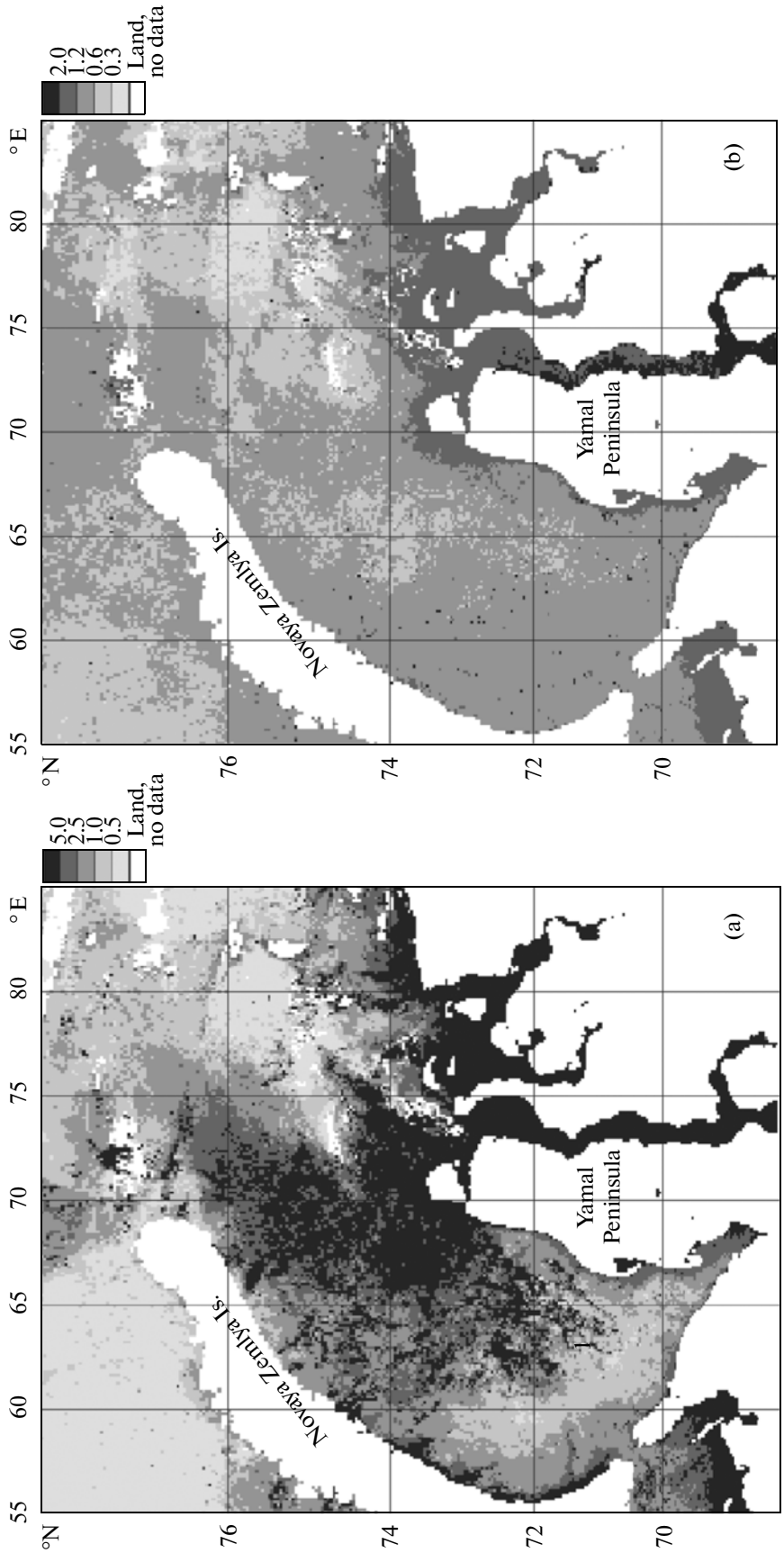

Fig. 2. Spatial distribution of the chlorophyll concentration based on the standard algorithm for the MODIS-Aqua scanner (a) and on the regional algorithm for the Kara Sea (b). The scanner's data were averaged over the period of September 1–26, 2007.

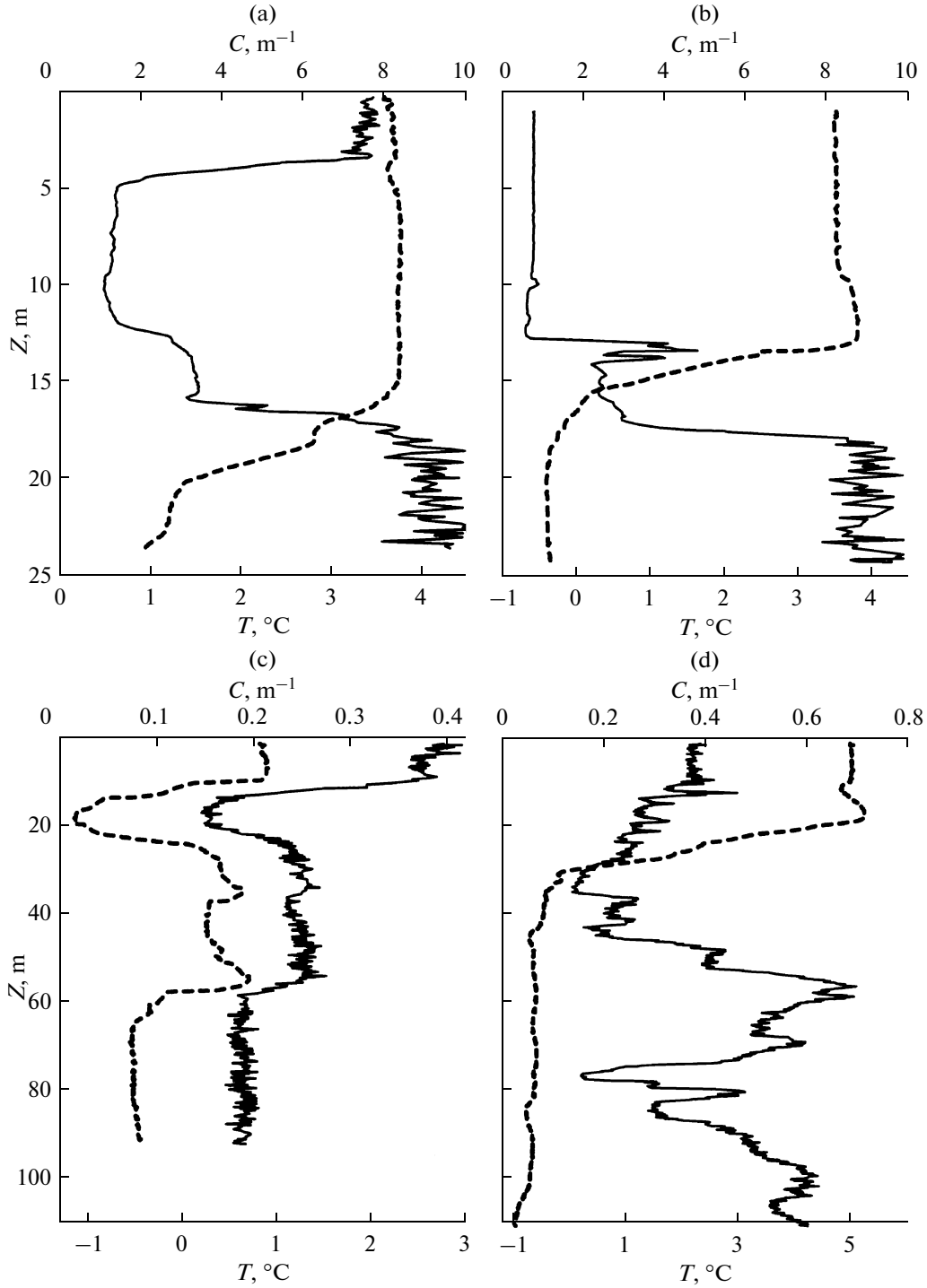

Fig. 3. Vertical profiles of the attenuation coefficient C (solid) and the temperature T (dashed) at stations 4999 (a), 5000 (b), 4989 (c), and 4958 (d). See the text for details.

Figure 1 allows us to compare the distributions of the b_{bp} and SST in the Kara Sea. This issue is considered at length in [7], where the authors analytically treat the concentration of the total suspended matter (TSM) derivable from the b_{bp}. Therefore, we dwell here only on the basic questions.

The largest b_{bp} occurred in the Ob gulf and Yenisei bay due to the incoming suspended matter of river origin. The Ob–Yenisei current transports the turbid waters from these bays eastwards. Frontal zones occur at the boundaries of the Ob gulf and the Yenisei bay, where the b_{bp} estimates drop by an order of magnitude.

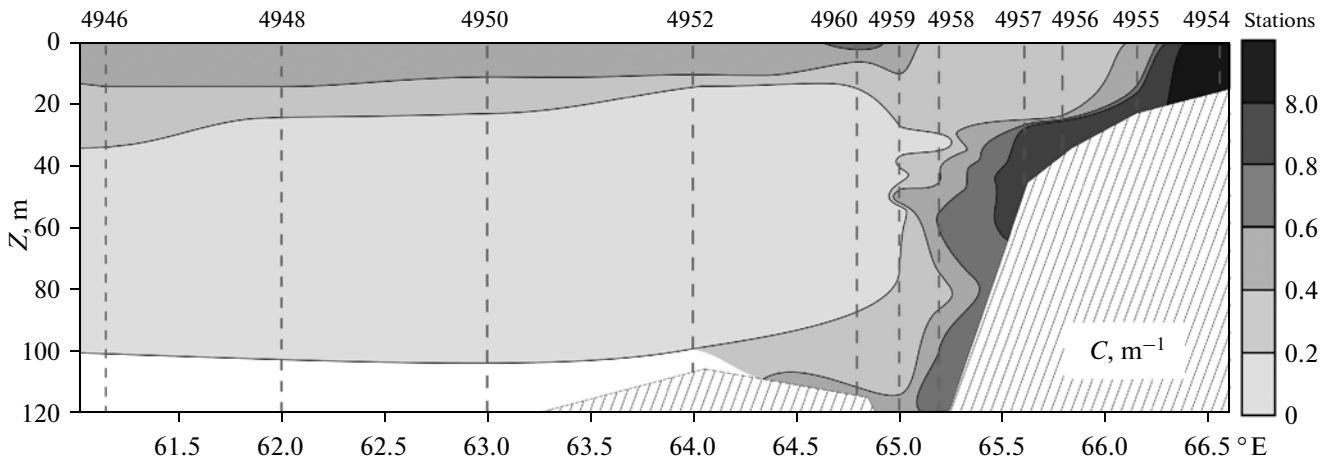

Fig. 4. Distribution of the attenuation coefficient C in the Yamal section. The half-tone scale of C is given in m^{-1}.

Turbid waters occur in Baidaratskaya Bay and within a narrow strip near the west coast of the Yamal peninsula too. In this case, higher b_{bp} emerge as a result of the resuspension of the bottom sediments by the tidal currents and the penetration of turbid waters from Baidaratskaya Bay. The SST distribution gives additional evidence of the propagation of relatively warmer waters of Baidaratskaya Bay along the Yamal margin. The b_{bp} estimates sharply decrease to the west of the Yamal margin, where the Yamal current transports relatively transparent waters from the south. Their temperature is lower against the margin zone. Next, the scattering values increase, which may be due to the higher biological productivity in the area. The surface waters exhibit here higher temperatures, supposedly because of the penetration of warmer waters from Baidaratskaya Bay.

The narrow strip of waters of higher turbidity observable near the eastern margin of the Novaya Zemlya Islands is seemingly due to the uptake of matter of terrestrial origin with the outwash from the shore. A region of colder waters corresponds to this strip on the SST map and relates to a local water upwelling along the eastern margin of the Novaya Zemlya Islands [9]. Thus, there is rather close correspondence between the distributions of the light scattering and the SST.

The distributions of the chlorophyll concentration C_{chl} based on the standard algorithm (for the MODIS-Aqua color scanner) and the Kara Sea's regional algorithm are compared in Fig. 2. As predicted, the standard algorithm substantially overestimates the chlorophyll concentration in reference to the regional one and to the shipborne measurements. The regional algorithm gives the best correlation with the chlorophyll determinations C_{chl} in the water samples, but, as noted above, this algorithm must be regarded as a preliminary one. The distribution of the chlorophyll concentration as found with the regional algorithm exhibits approximately the same patterns that are characteristic of the suspended matter distribution.

4. THE DISTRIBUTION OF THE OPTICAL CHARACTERISTICS IN THE KARA SEA FROM THE SHIPBORNE MEASUREMENTS

The accomplished measurements provide evidence of a large range of variability of the optical characteristics in the Kara Sea regions under study. This appears quite natural, since the water turbidity is high in the Ob gulf and Yenisei bay thanks to the river run-off, while the primary production of the open sea is low and the river run-off effects sharply fall. The Secchi disk's visibility depth A_W changed from 16–17 m in the open sea regions to 0.5 m in the Ob gulf, while the light attenuation coefficient C varied from 0.11–0.12 m^{-1} in the west (station 4952) and north (station 4948) of the sea to 10 m^{-1} in the Ob gulf. As for the fluorescence of the chlorophyll and DOM, 15-fold and 6-fold changes in their intensities were recorded, respectively.

The strong variability in the horizontal and the vertical and the sharp changes in the magnitudes when passing the frontal zones represent another distinction of the hydro-optical characteristics.

The vertical structure of the attenuation coefficient exhibited extreme diversity too. The most characteristic examples are given in Fig. 3. The vertical distribution of the attenuation coefficient typical of the regions of intense mixing of the riverine and marine waters took place at station 4999 near the boundary of the Ob gulf. The extremely turbid riverine waters occupied the upper 5 m thick layer (here, the attenuation coefficient C was as high as 7.5 m^{-1}). Much more transparent waters occupy the underlying layer, where

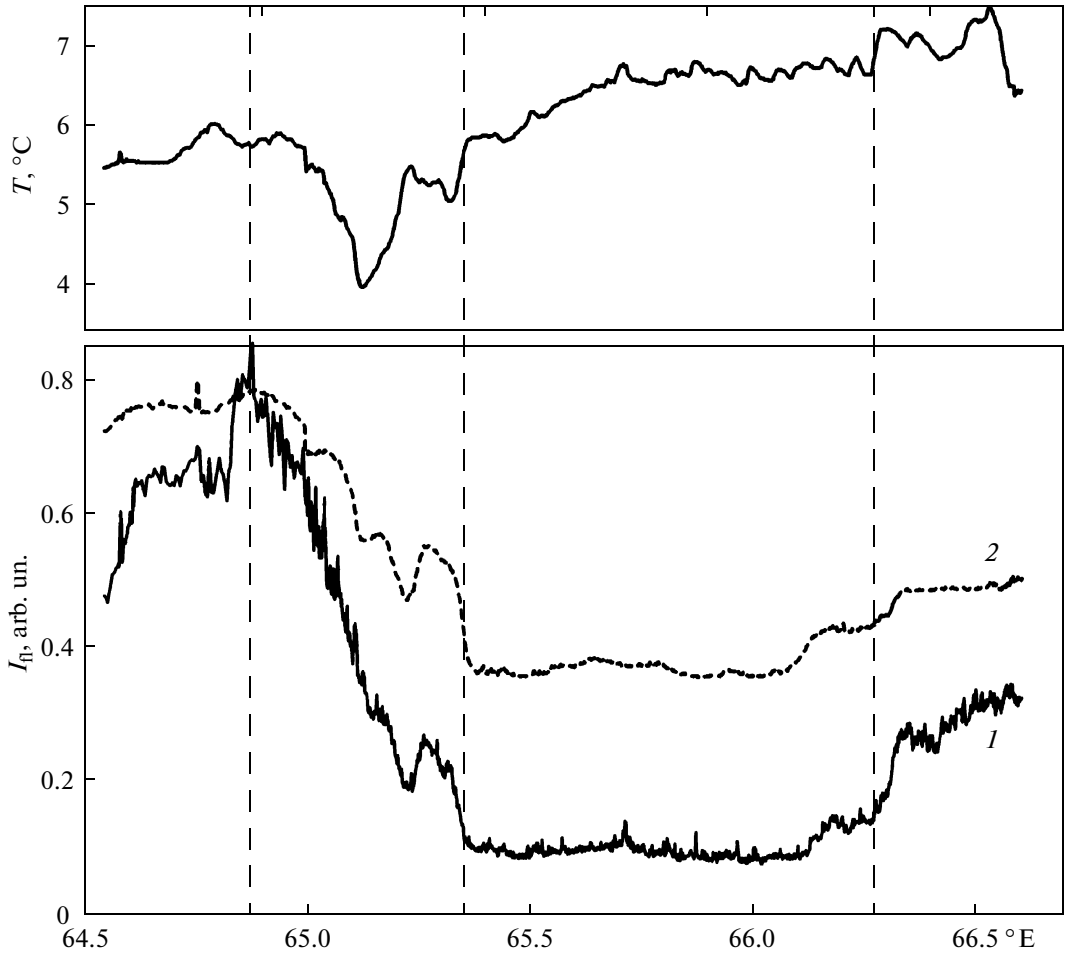

Fig. 5. Distribution of the SST (top) and fluorescence intensities (bottom) in the Yamal section between stations 4952 and 4954. *1*, chlorophyll fluorescence; *2*, DOM fluorescence. The dashed vertical lines show the localization of the frontal zones in the section.

the riverine and marine waters mix. A bottom nepheloid layer occurs near the sea floor, where water transparency is as low as in the upper layer thanks to the resuspension of the bottom sediments by the tidal currents. The occurrence of a bottom nepheloid layer is typical of most of the Kara Sea areas. At station 5000, which is just northwards of station 4999, the marine and riverine waters mix in the vertical, which results in a homogeneous layer 15 m thick. The bottom nepheloid layer underlies the latter.

The vertical $C(z)$ profile recorded at station 4989 in the area of the St. Anna Trench exhibits a slightly turbid surface layer (its C values are considerably lower than those in the Ob gulf) and more transparent underlying waters of intricate vertical structure. Noteworthy also are the correlated changes of the attenuation coefficient and the temperature in the vertical. The occurrence of inversions in the temperature profiles indicates intrusion processes in the area where the northerly Barents Sea waters interact with the easterly Novaya Zemlya current [9]. The intricate vertical structure of the attenuation coefficient is inherent to a frontal zone west of the Yamal Peninsula (station 4958). Apparently, this frontal zone is a result of the interaction between the waters of the open Kara Sea and the turbid coastal waters from Baidaratskaya Bay, whose turbidity is also contributed to by the tidal resuspension of the bottom sediments. The narrow strip of turbid waters at the western Yamal margin is easy to see in the satellite images (Fig. 1a).

Naturally, these examples don't exhaust the diversity of the vertical profiles of the attenuation coefficient. Nonstratified or slightly stratified waters were found in a number of regions (with the Ob gulf and the northern Kara Sea as respective examples). In general, the notion of the stratification of the attenuation coefficient in the Kara Sea agrees with the findings of the expedition in 1993 [4].

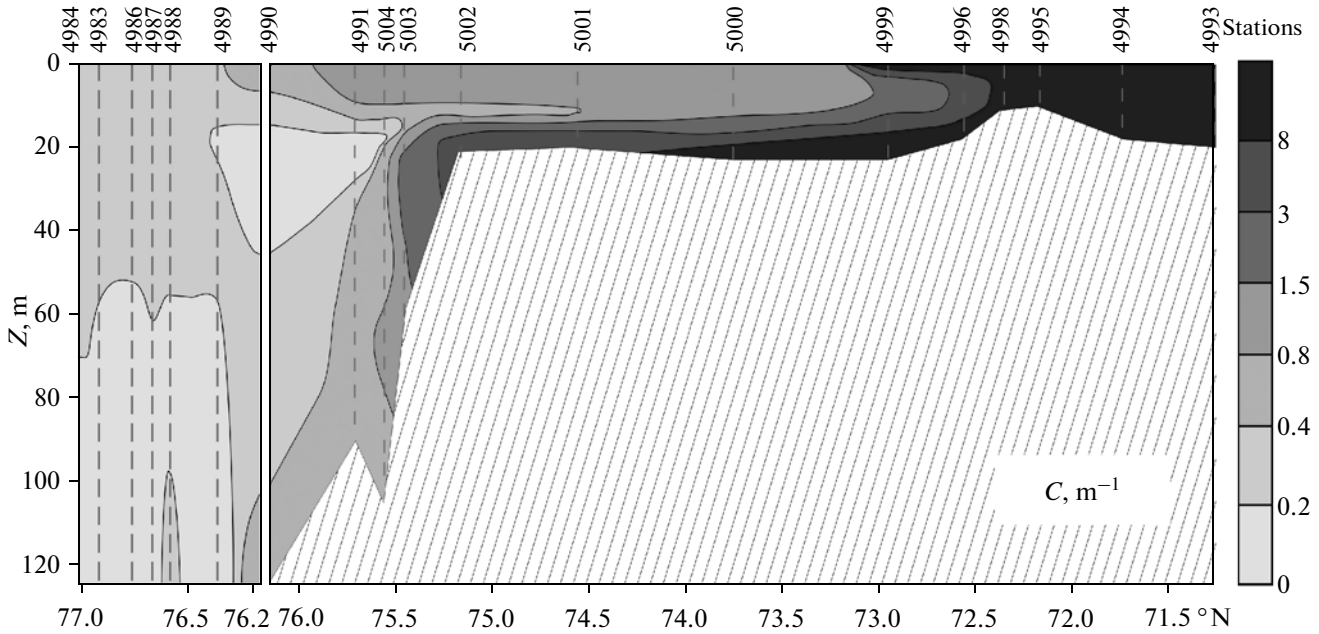

Fig. 6. Distribution of the attenuation coefficient C in the Ob section (from the Ob river to the St. Anna Trench). The half-tone scale of C is given in m^{-1}.

The Distribution of the Optical Characteristics in the Yamal Section

The shipborne measurements of the distributions of the attenuation coefficient C were performed mainly in the Yamal (1) and Ob (2) sections (Fig. 1).

Figure 4 shows the spatial distribution of the magnitude of C in the Yamal section from data of the PUM transmissometer. Figure 5 gives the distributions of the fluorescence intensity of the C_{chl} and DOM, along with the SST, in the eastern sector of the same section from station 4952 to station 4954.

The largest magnitudes of the attenuation coefficient measured about 7 m^{-1} both in the surface and bottom layers and occurred at station 4954, which is the closest to the shore. Here, the attenuation coefficient's stratification was weak. Supposedly, the high turbidity of the waters in this area is attributable to the bottom and shore abrasion, which is caused by the tidal currents, and to the transport of turbid waters from Baidaratskaya Bay. The satellite data confirm the occurrence of turbid waters at the Yamal margins. The relatively low intensities of the fluorescence of the C_{chl} and DOM indicate the dominant contribution of the suspended matter concentration to the turbidity of the water of the coastal zone.

The attenuation coefficient drops by an order of magnitude offshore. The estimates of the attenuation coefficient only slightly change at stations 4955–4959 in the surface layer and at the depths down to 20 m (C measures about 0.3 m^{-1}) and nepheloid layer occurs near the bottom (C is higher 1 m^{-1}). According to the hydrology data, the Yamal current flows here and transports relatively transparent waters from the south [9]. This strip is also easy to see on the satellite maps. The intricate stratification of the attenuation coefficient caused by intrusion processes takes place in the area where the turbid coastal waters mix with the clearer waters of the Yamal current. The distributions of the fluorescence of the C_{chl} and DOM visualize the frontal zones at the current's boundaries. Next, the attenuation coefficient grows in the upper layer and remains almost unchanged until the end of the section. An exception is represented at station 4960 with the magnitudes of C exceeding 1 m^{-1} in the surface layer 5 m thick. Probably, this is due to the occurrence of an area of enhanced bioproductivity. As follows from Fig. 5 and in accordance with [9], the maximum chlorophyll fluorescence intensity was observed at this location.

West of the station 4960, the stratification and magnitude of the attenuation coefficient exhibited low variability. Higher attenuation coefficient values occurred in the surface layer, which was due in part to the river water transport (the surface waters are slightly desalinated here [9]) and in part to the enhanced bioproductivity [12]. The increased suspended matter concentration is evident in this area from the satellite imagery too [7]. Waters of fairly high transparency (close to that of the open ocean) occurred at the depth levels below 20–30 m.

The Secchi disk's visibility depth Z_W fluctuated within 11–12 m in the section but became as high as

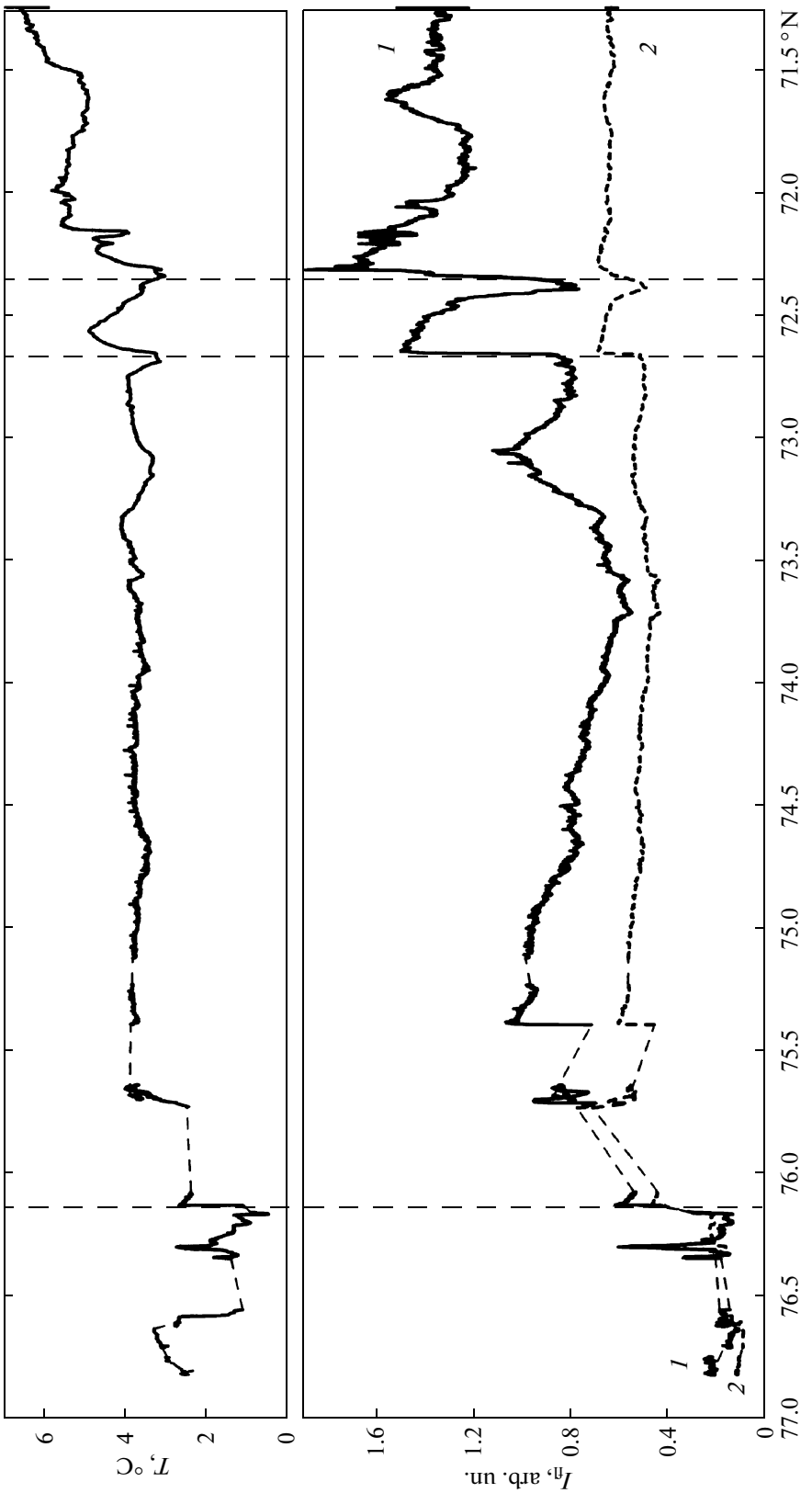

Fig. 7. Distributions of the SST (top) and the fluorescence intensities (bottom) in the Ob section (from the Ob river to the St. Anna Trench). *1*, chlorophyll fluorescence; *2*, DOM fluorescence. The dashed segments correspond to the gaps in the PLF measurements at the station sites. The dashed vertical lines show the localization of the frontal zones in the section.

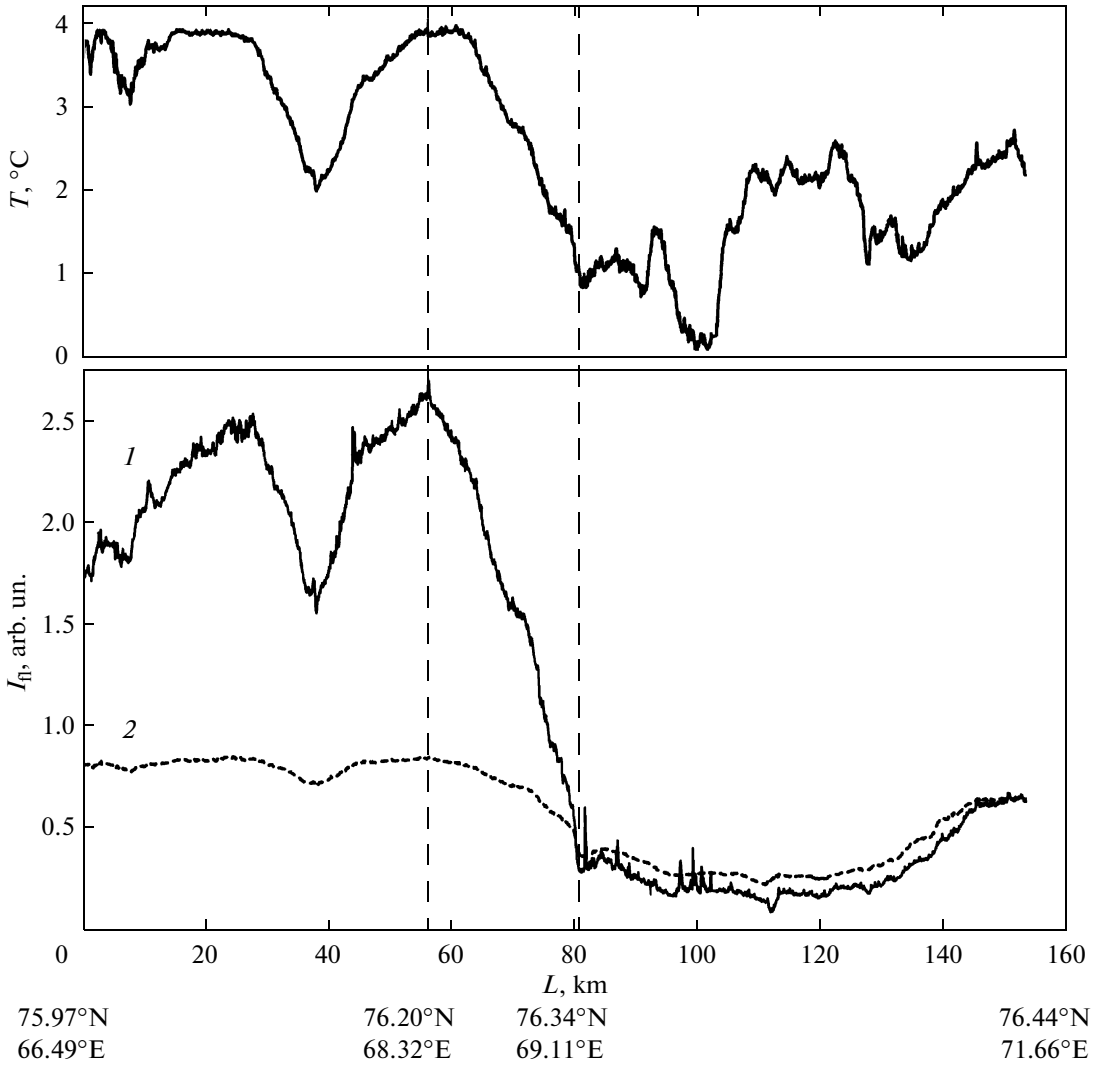

Fig. 8. Distributions of the SST (top) and fluorescence intensities (bottom) in section 3. *1*, chlorophyll fluorescence; *2*, DOM fluorescence.

15 m at station 4957. The estimate of the Z_W dropped below 1 m at the eastern end of the section occupied by very turbid waters.

The Distribution of the Optical Characteristics in the Ob Section

The distribution of the attenuation coefficient in the Ob section from the river Ob to the St. Anna Trench is given in Fig. 6, while Fig. 7 shows the distributions of the intensities of the fluorescence of the chlorophyll "a" and the DOM and SST. This section is similar in part to the section occupied in 1993 by the R/V *Dmitriy Mendeleev* during cruise 49.

The section starts in the OB Bay. Here, the magnitude of the attenuation coefficient is about 7–8 m^{-1}, being the largest for the whole section thanks to the influence of the river runoff, but the stratification is weak due to the vertical mixing. At the boundary of the Ob gulf close to station 4999, a frontal zone occurs, where the water transparency sharply increases and a three-layer stratification appears involving the upper turbid waters, the more transparent underlying layer, and the bottom nepheloid layer. The localization of the frontal zone is clearly indicated in the distributions of the fluorescence intensity. The vertical dashed lines indicate the positioning of the fronts in Fig. 7 (As follows from the analytical treatment of the data, the occurrence of two fronts is attributable to the intersection of two meanders of the frontal zone).

North of station 4999 in the area of a shallow shelf 20–25 m deep, the turbid river waters mix in the vertical with the more transparent marine waters, which resulted in the two-layer stratification of the attenua-

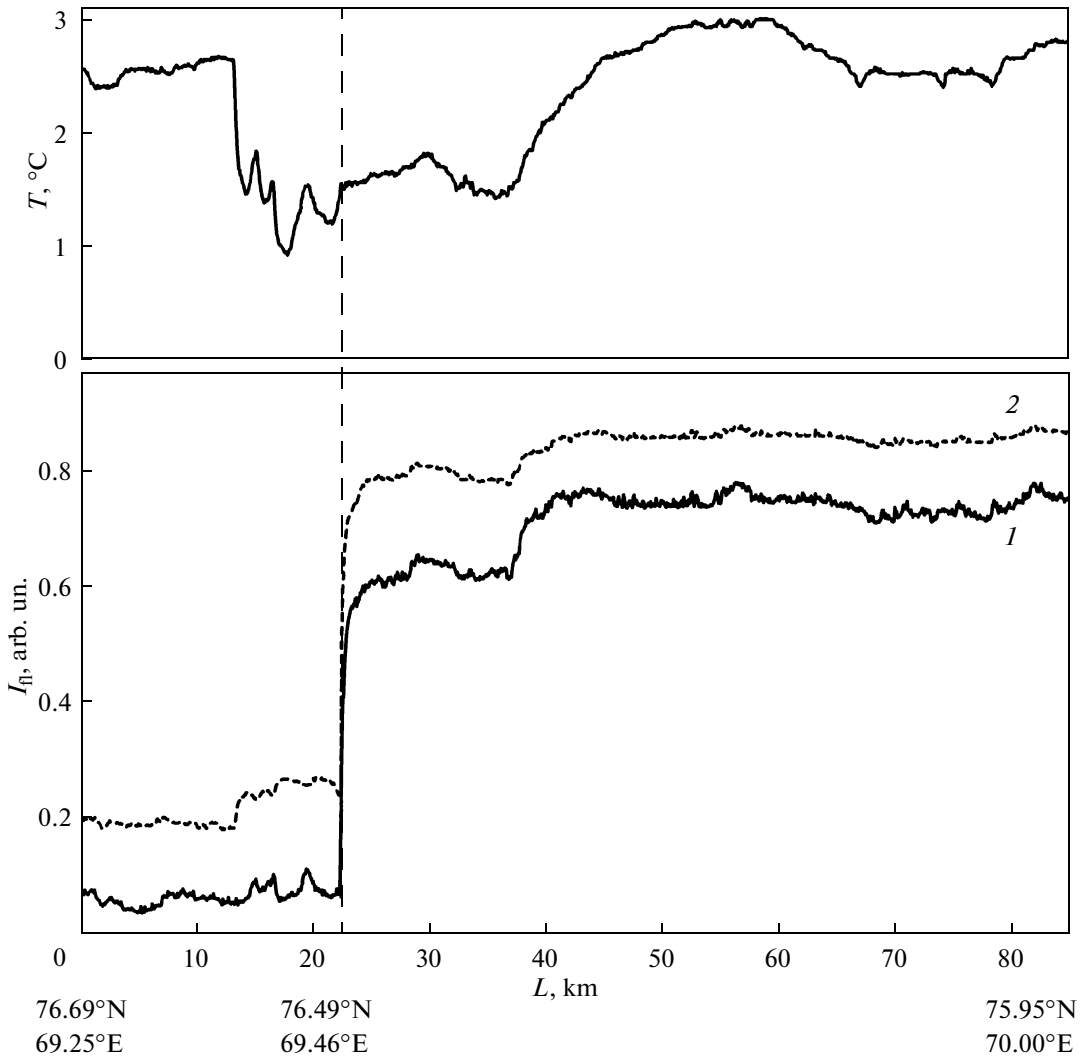

Fig. 9. Distributions of the SST (top) and the fluorescence intensities (bottom) in section 4. *1*, chlorophyll fluorescence; *2*, DOM fluorescence.

tion coefficient involving the quasi-homogenous surface layer and the bottom nepheloid layer. The upper 10 m thick layer is occupied by desalinated waters of higher turbidity thanks to the river runoff. Saline waters underlie this layer, while the turbidity increase in the bottom layer results from the tidal motions. The water transparency grows northwards both in the surface and bottom layers.

Such stratification is a feature of the whole shelf part of the section to the point of the depth of about 100 m, where three-layer stratification appears. The upper 10 m thick layer is rather turbid because of the river runoff's influence (the hydrological measurements point to the freshening of this layer) and the phytoplankton's growth, which results in a higher attenuation coefficient in the upper layer leading to the stratification typical of high latitudes. Waters of high transparency close to oceanic waters in the magnitude of the attenuation coefficient occur below the upper layer. A bottom nepheloid layer occurs here too, but it is not as strong as in the near-estuary area. Waters of higher transparency occurred at depths of 20–40 m between stations 4989 and 4991, where a temperature minimum existed. Here, the attenuation coefficient and the temperature covaried in the vertical (see Fig. 3c). Apparently, this anomaly points to intrusion processes in the area of the interaction of the Barents Sea waters propagating from the north and the Novozemel'skoye Current [9].

The water transparency sharply grows north of station 4989 where the frontal zone occurs. The PLF data indicate the latter and demonstrate a several times decrease in the intensity of the fluorescence of the chlorophyll and the DOM (a dashed line marks this front in Fig. 7). The optical front coincides with the thermal front where the temperature jumps by 1.5°C.

This frontal zone occurs at the limit of the river runoff's influence (the salinity increases in this area). Notice that frontal zones of lesser intensity were found in the section too (Fig. 7).

The Secchi disk's visibility depth Z_W south of the frontal zone near station 4999 was as low as 0.6–0.8 m. The Z_W ranged from 4 to 7 m in the middle of the section between the frontal zones. The Z_W reached 14–15 m north of station 4989.

By and large, the results from the Ob section agree with the data of the expedition in 1993 [4]. The distribution of the attenuation coefficient in the surface layer is consistent with the satellite data (Figs. 1 and 2).

The Northern Boundary of the Desalinated Waters' Area

The area of freshened waters of the Novozemel'skoye Current in the vicinity of the northern tip of the Novaya Zemlya Islands and the St. Anna Trench borders the Barents Sea waters propagating from the north. As noted above, these water strongly differ in their optical properties, specifically, in the intensity of the fluorescence of the DOM and the chlorophyll. A low level fluorescence is typical of the Barents Sea waters, while the desalinated water exhibits considerably brighter fluorescence.

The survey's track crossed the boundary between the Barents Sea and the desalinated waters several times. The boundary appeared each time as a sharp front in the spatial distribution of the fluorescence intensities of the chlorophyll *a* and DOM. This front is easy to see in Fig. 7. Figures 8 and 9 give other examples of the frontal interfaces at the desalinated water boundary. The distributions of the chlorophyll *a* and DOM, along with the SST, in these figures were plotted from the PLF data for Sections 3 and 4, whose localizations are given in Fig. 1.

The frontal zone in section 3 exhibits more than a 10-fold decrease in the chlorophyll fluorescence intensity and more than a 2-fold decrease in the DOM fluorescence. At that, the pattern of the covariance of the fluorescence intensity and the SST changes too. In the desalinated waters, the fluorescence intensities covary with the SST. After crossing the frontal interface, the fluorescence intensity distributions become flat against the background of the fairly strong changes in the SST.

We obtained the most impressive pattern of the distributions of the fluorescence intensities of the chlorophyll and the DOM near the Novaya Zemlya margin when crossing the frontal zone at a right angle during Section 4 occupied on September 1–2, 2007. The survey's itinerary took into account the results of the earlier studies and concurrent maps of the SST and the optical characteristics. Passing into the desalinated waters resulted in a 6-fold and a 4-fold increase in the chlorophyll and DOM fluorescence intensities, respectively. The ship's tracking of the maximal gradient of the fluorescence intensity was less than 1 km long. It is important to note that a sharp "fluorescence" front occurred in the background of a moderate SST jump, while small spatial variations of the fluorescence intensities accompanied much stronger temperature changes on both sides of the front.

5. CONCLUSIONS

Our measurements provide evidence of the large range of the variability of the optical characteristics in the Kara Sea caused by the strong influence of the river runoff and the relatively low biological productivity. The largest magnitudes of the optical characteristics occurred in the areas influenced by the river runoff (the Ob gulf and the Yenisei and Baidaratskaya bays). This factor is at its minimum in the northern and western Kara Sea; hence, the minimal attenuation coefficient estimates are characteristic of these areas. The distributions of the optical properties feature frontal zones where the optical characteristics jump several-fold. The distribution of the optical properties is tightly bound to the hydrology and the current structure of the Kara Sea. The satellite observations are consistent with the data of the shipborne measurements.

ACKNOWLEDGMENTS

The data of the MODIS-Aqua color ocean scanner used in our study were obtained from the DAAC GSFC data center of NASA.

The authors are grateful to Yu.I. Ventskut, A.V. Grigoriev, B.A. Gureev, B.R. Taskaev, and O.V. Prokhorenko for help in the measurements and data processing and to S.V. Mosharov for data on the chlorophyll concentration.

This work was supported by the federal targeted program entitled Research and Development in Priority Fields of the Science and Technology Complex of Russia for 2007–2012 (state contract no. 02.515.11.5037).

REFERENCES

1. V. A. Artem'ev, V. R. Taskaev, V. I. Burenkov, and A. V. Grigor'ev, "Universal Compact Gauge of Vertical Distribution of the Light Attenuation Index," in *Multidisciplinary Studies of the World Ocean: The Meridian Project (Atlantic Ocean)* (Nauka, Moscow, 2008), pp. 165–172 [in Russian].
2. V. A. Artem'ev, V. I. Burenkov, A. V. Grigor'ev, et al., "Optics," in *The Pechora Sea: Multidisciplinary Studies* (MORE, Moscow, 2003), Ch. 3, pp. 247–262 [in Russian].

3. V. I. Burenkov, V. M. Kuptsov, V. V. Sivkov, and V. P. Shevchenko, "Spatial Distribution and Size Composition of Suspended Matter in the Laptev Sea in August–September 1991," Okeanologiya **37** (6), 920–927 (1997) [Oceanology **37** (6), 831–837 (1997)].

4. V. I. Burenkov, Yu. A. Gol'din, B. A. Gureev, and A. I. Sud'bin, "The Main Ideas on the Distribution of Optical Characteristics of the Kara Sea," Okeanologiya **35** (3), 376–387 (1995).

5. V. I. Burenkov, S. V. Ershova, O. V. Kopelevich, et al., "An Estimate of the Distribution of Suspended Matter in the Barents Sea Waters on the Basis of the SeaWiFS Satellite Ocean Color Scanner," Okeanologiya **41** (5), 653–659 (2001) [Oceanology **41** (5), 622–628 (2001)].

6. V. I. Burenkov, S. V. Gladyshev, and Yu. A. Gol'din, "Variability of Optical Characteristics on the Section SR-2 in Southern Atlantics," in *Multidisciplinary Studies of the World Ocean: the Meridian Project, Atlantic Ocean* (Nauka, Moscow, 2008), pp. 173–178 [in Russian].

7. V. I. Burenkov, Yu. A. Gol'din, and M. A. Kravchishina, "Distribution of Particulate Matter Concentration in the Kara Sea in September 2007 Based on Onboard and Satellite Observational Data," Okeanologiya **50** (5), 842–849 (2010).

8. B. A. Gureev, Yu. A. Gol'din, and Yu. I. Ventskut, "Flow Laser Fluorometer," in *Multidisciplinary Studies of the World Ocean: Multidisciplinary Studies of the World Ocean: the Meridian Project, Atlantic Ocean*, (Nauka, Moscow, 2008), pp. 189–195 [in Russian].

9. A. G. Zatsepin, "Hydrophysical Characteristic of the Kara Sea," in *Report on Work in Cruise 54 of R/V "Akademik Mstislav Keldysh*," Vol. 2: *Team Leader Reports* (IO RAN, Moscow, 2008), pp. 2–10 [in Russian].

10. O. V. Kopelevich, V. I. Burenkov, and S. V. Sheberstov, "Development and Use of Regional Algorithms for Calculation of Bio-Optical Characteristics of Russian Seas Based on Satellite Color Scanners," in *Modern Problems of Remote Probing of the Earth from Space*, (OOO Azbuka, Moscow, 2006), issue 3, Vol. II, pp. 99–105 [in Russian].

11. V. A. Matyushenko, I. K. Popov, and I. L. Misyuchenko, "Spatial Distribution of the Attenuation Index in Waters of the Kara Sea," Dokl. Akad. Nauk **2** (3), 403–406 (1995).

12. I. N. Sukhanova, M. V. Flint, S. A. Mosharov, et al., "Structure of Phytoplanktonic Communities and Primary Production in the Ob River Estuary and Adjacent Kara Shelf," Okeanologiya **50** (5), 785–800 (2010).

13. O. V. Kopelevich, V. I. Burenkov, S. V. Sheberstov, et al., "Application of SeaWiFS Data for Studying Variability of Bio-Optical Characteristics in the Barents, Black, and Caspian Seas," Deep-Sea Res. II **51**, 1063–1091 (2004).

14. O. V. Kopelevich, V. I. Burenkov, S. V. Sheberstov, et al., "Continuation of Long-Term Series of Data in the Bio-Optical Characteristics of the Russian Seas from Satellite Ocean Color Data," in *Proceedings of IV International Conference: Current Problems in Optics of Natural Waters (ONW' 2007), Nizhny Novgorod, September 11–15, 2007* (Nizhny Novgorod, 2007), pp. 75–78.

15. O. V. Kopelevich, V. I. Burenkov, S. V. Vazyulya, et al., "Bio-Optical Characteristics of the Seas of Russia from Data of the SeaWiFS Satellite Ocean Color Scanner," CD-ROM (SIO RAS, Moscow, 2007).